Rapid thermal processing of CuInSe2 electroplated precursors for CuIn(S,Se)2-based thin film solar cells

Cédric Broussillou, G. Savidand, L. Parissi, J.S. Jaime-Ferrer, P.P. Grand, Cédric Hubert, O. Roussel, E. Saucedo, V. Bermudez, Michel Andrieux, et al.

Available online at www.sciencedirect.com
ScienceDirect
Energy Procedia 2 (2010) 9–17
Energy Procedia
www.elsevier.com/locate/procedia

European Materials Research Society Spring 2009 Conference - Symposium B

Rapid Thermal Processing of $CuInSe_2$ Electroplated Precursors for $CuIn(S,Se)_2$-Based Thin Film Solar Cells

C. Broussillou*[a,d], G. Savidand[b], L. Parissi[a], J.S. Jaime-Ferrer[a], P.P. Grand[a], C. Hubert[a], O. Roussel[a], E. Saucedo[a], V. Bermudez[a], M. Andrieux[c], M.H. Berger[d], M. Jeandin[d]

[a]*Nexcis, Photovoltaic technology, 190 avenue Célestin Coq, 13106 Rousset, France*
[b]*Institute of Research and Development on Photovoltaic Energy IRDEP (EDF/CNRS/ENSCP), 6 Quai Watier, 78401 Chatou Cedex, France*
[c]*Univ. Paris Sud 11, LEMHE-ICMMO, CNRS UMR 8182,Bât. 410, 91405 Orsay, France*
[d]*MINES ParisTech, Centre des Matériaux, CNRS UMR 7633,BP 87 91003 Evry Cedex, France*

Received 1 June 2009; received in revised form 1 December 2009; accepted 20 December 2009

Abstract

During the elaboration of standard CISEL™ cells, electroplated $CuInSe_2$ precursors undergo a rapid thermal processing (RTP) in a sulfur-containing atmosphere to promote grain growth and enable sulfurization of the precursor. The aim of this work is to show how structural and morphological properties of the $CuIn(S,Se)_2$-based solar cells can be modified with RTP parameters, namely temperature, heating rate, and sulfur addition. X-ray diffractograms show that the preferential (112) orientation of the electrodeposited $CuInSe_2$ precursor is maintained after annealing but the coefficient of crystallographic texture can be modified with specific RTP parameters. It is also shown that the quantity of sulfur incorporated in the chalcopyrite lattice can be controlled and reaches almost pure $CuInS_2$ according to the sulfur quantity used during the RTP. Another effect of the RTP annealing is to form a $Mo(S,Se)_2$ layer which can lead to a quasi-ohmic contact between the molybdenum and the absorber. The properties of the $Mo(S,Se)_2$ buffer layer are also studied according to the process parameters and an increase of the annealing temperature or of the sulfur concentration tends to increase the thickness of this layer.

Keywords: Rapid thermal processing; chalcopyrite; $CuInS_2$; $CuInSe_2$; structural properties; morphology; sulfurization

1. Introduction

Chalcopyrite-based Cu(In,Ga)(S,Se) thin film solar cells are made using many different processes ranging from direct evaporation of all the elements [1], sputtering of the cations which then react with chalcogens [2], spray pyrolisis [3], or two steps electrodeposition-annealing process [4]. A lot of work has already been published concerning chalcopyrite materials since they are some of the most promising semiconductors to make cost-efficient solar cells due to low production cost and high cells efficiency as has been demonstrated by Repins et al [5]. The use

* Corresponding author. Tel.: +33 1 60 76 30 60; fax: +33 1 60 76 31 50.
E-mail address: cedric.broussillou@mines-paristech.fr.

1876-6102 © 2010 Published by Elsevier Ltd
doi:10.1016/j.egypro.2010.07.004

of electrodeposited precursors is even more interesting than physical vapour deposition processes to achieve low production costs because the deposition of the precursor is done at ambient pressure and temperature, using industrial equipment much less expensive than sputtering coaters or evaporators.

The as-electrodeposited $CuInSe_2$ precursor material is nano-crystallized and does not exhibit good optoelectronic properties, thus an annealing step is necessary to promote grain growth and enable the formation of effective absorbers. The annealing step is closely linked with the electrodeposition step since the secondary phases such as Cu-Se binaries, elemental Se or ordered vacancy compounds (OVC) that form during the precursor deposition have been shown to greatly influence the structure and morphology of the absorbers [6]-[7]. The purpose of this work is to analyze the effect of annealing parameters such as temperature, heating rate, and sulfur pressure on the structure and morphology of the $CuIn(S,Se)_2$ layer formed after rapid thermal processing in a sulfur containing atmosphere. During the rapid thermal processing of $CuInSe_2$ precursors, the formation of a large $Mo(S,Se)_2$ intermediate layer has been observed at the interface between molybdenum and $CuIn(S,Se)_2$ and the effect of the annealing parameters on this layer are also studied.

2. Experimental

$CuIn(S,Se)_2$ absorber layers were grown on Mo-coated soda-lime glass substrates with a two-step process. A nanocrystalline precursor layer of $CuInSe_2$ was first deposited by electrodeposition on a molybdenum cathode in an acidic bath containing Cu(II), In(III) and Se(IV) electroactive species. The electrodeposition parameters were tuned so that the film composition achieved an overall Cu/In ratio and a stoichiometry 2Se/(Cu+3In) respectively equal to 1.20 and 1.24. The composition of the precursors was determined using a Fischerscope X-ray XVD-SD apparatus. The precursors were then annealed in a sulfur atmosphere with a rapid thermal process using IR heating lamps. The maximum annealing temperature was set at three different values being 550°C, 600°C and 650°C. The heating rate for the lower temperature (550°C) was varied between 1.8°C/s and 8.8°C/s. A 60-second holding time at maximum temperature was used for all heating ramps after which an unassisted cooling to 100°C was allowed before taking the samples out. The sulfur pressure during the RTP was varied by changing the mass over volume ratio from 0.01 g/L to 6 g/L. The real sulfur pressure in the reaction chamber could not be precisely calculated because part of the sulfur reacted with the $CuInSe_2$ precursor to form a quaternary $CuIn(S_{1-x}Se_x)$ compound, thereafter named CIS for simplicity, but we assumed that the higher the initial ratio, the higher the maximum sulfur pressure was during the annealing. In all cases, the sulfur quantity was always above stoichiometry to ensure that there was enough sulfur in the reaction chamber to possibly replace all the selenium present in the precursor.

After annealing and sulfurization, a few chosen samples followed the standard CIS-based process at the Institute of Research and Development on Photovoltaic Energy (IRDEP) in order to be completed into the solar cells. This consisted in a cyanide etching to remove Cu(S,Se) binaries which form on the absorber surface during annealing [8], followed by the formation of a CdS buffer layer by chemical bath deposition. Both undoped and aluminium-doped zinc oxide was then sputtered on top as window layer.

Samples were characterized by means of X-Ray diffraction (XRD), Raman spectroscopy, and scanning electron microscopy (SEM) using a Hitachi TM-1000 microscope for surface observation and a field emission gun Zeiss Gemini DSM 982 microscope for cross-section observation. Raman microprobe measurements were made using a HR800-UV Horiba-Jobin Yvon spectrometer coupled with an Olympus metallographic microscope. The spectra were measured on the absorber using as excitation the red line of an He-Ne laser (λ=632.8nm). The spectra obtained were fitted with Gaussian-Lorentzian profiles using the LabSpec software. Eventually, XRD analyses were performed in the θ-2θ Bragg-Brentano geometry with a Panalytical X'Pert Pro MRD diffractometer using the Kα emission line of a copper anticathode.

3. Results and Discussion

3.1. Effect of temperature

Fig. 1 shows SEM surface micrographs after cyanide etching taken from samples annealed at three maximum temperatures 550°C, 600°C and 650°C with an 8.8°C/s heating rate and a sulfur concentration of 1 g/L.

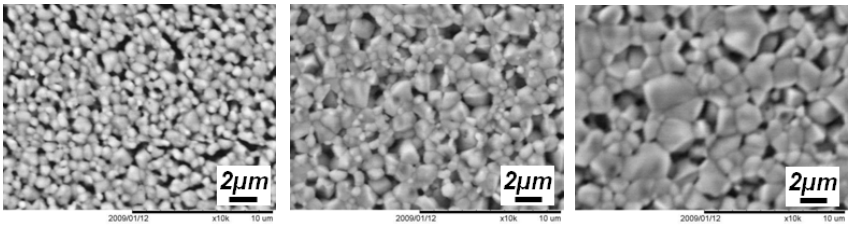

a) b) c)

Fig. 1 : SEM top-view micrographs of $CuIn(S,Se)_2$ absorbers annealed at a) 550°C, b) 600°C, c) 650°C maximum temperature after cyanide etching

Samples annealed at higher temperature have larger grains due to a more pronounced coarsening during grain growth (Fig. 1). For higher annealing temperature some grains are favored and tend to grow more than others resulting in a less homogeneous morphology showing both small and large grains while at 550°C all grains have almost the same size. This is typical of preferential grain growth where a family of crystallites oriented in a specific way is favored over other crystallographic orientations. This observation can be related to the diffractograms of Fig. 2 which show that the sample annealed at 650°C is the one with the highest (112) orientation of the chalcopyrite phase. To better point out this preferential orientation, the chalcopyrite reflections were identified and fitted with pseudo-voigt profiles to deduce the intensities and estimate the texture coefficient (TC) as described in [9]. TC(112) values larger than 1 indicate a preferred orientation of the material with (112) dense planes parallel to the sample surface.

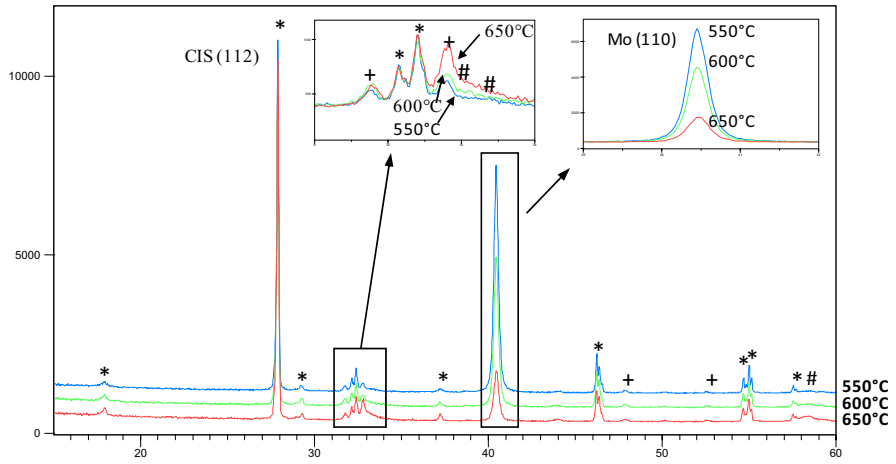

Fig. 2 :X-Ray diffractograms of samples annealed at 550, 600 and 650°C maximum temperature. The CIS phase is marked with asterisks, the CuS covellite with + signs and $Mo(S,Se)_2$ with #

TC(112) increases from 2.0 to 2.1 and up to 2.4 for the maximum annealing temperature of 550°C, 600°C and 650°C respectively. This correlates well with the SEM micrographs and means that the (112)-oriented grains are favored during grain growth and grow at the expense of others which tend to disappear all the more as the annealing temperature is higher. When the maximum annealing temperature increases, there is very little peak-refinement of the CIS reflections even though the grains coarsen significantly. This can be explained considering that CIS grains seen by SEM include a large number of twins [10] and an increase of the grain size is not necessarily accompanied by a refinement of the XRD reflections.

Increasing the annealing temperature also has an effect on the $Mo(S,Se)_2$ layer that forms between the molybdenum and CIS layer. The intensity at 33° next to the (004)/(200) reflections of CIS rises with the temperature because of the hexagonal $Mo(S,Se)_2$ (100) and (101) reflections respectively at 32.7° and 33.5° (insert in Fig. 2). This increase of the diffracted intensity is due to an increase of the $Mo(S,Se)_2$ thickness as mentioned in [11], which is coherent with the drop of the (110) molybdenum noticed when the maximum annealing temperature goes from 550°C to 650°C. When the material is annealed at higher temperature, sulfur diffuses more easily through the CIS which results in more molybdenum being transformed into $Mo(S,Se)_2$ [12].

3.2. Effect of heating rate

Fig. 3 shows micrographs of samples after cyanide etching annealed at a temperature of 550°C, the heating rate being respectively set at 1.8°C/s, 2.4°C/s and 8.8°C/s with a sulfur concentration equal to 6 g/L. There is little morphological difference between the three samples; grains are small for all of them even though a small increase in average grain size from 200nm to 300nm can be observed when the material is heated faster. An image analysis of Fig. 3 SEM micrographs was used to calculate the percentage of surface voids and values equal to 15.4 %, 17.5 % and 20.1 % for the respectively, 1.8°C/s, 2.4°C/s and 8.8°C/s heating rates were found. Thus, when the heating rate increases, there is an increase in surface open porosity which goes along with the grain growth observed. The fact that an increase of the grain size is accompanied by an increase in the surface porosity is probably due to the high growth and sulfurization rate of the grains which grow from a few nanometers before annealing to hundreds of nanometers within only a few minutes. Furthermore there is a 12% decrease in lattice volume when the $CuInSe_2$ is transformed into $CuInS_2$ and this volume change is more easily accommodated when the heating rate is slower, thus resulting in less porosity for slower heating rates.

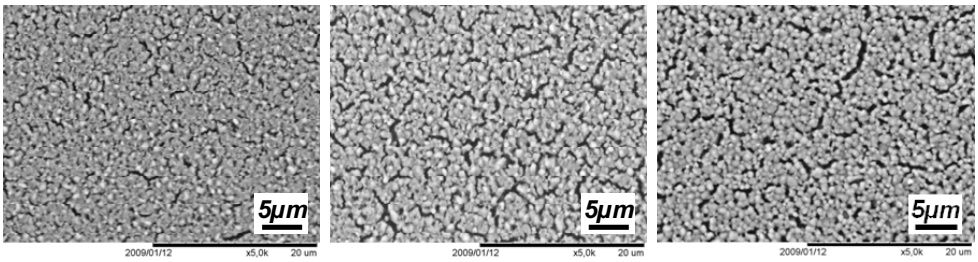

a) b) c)

Fig. 3 : SEM top-view micrographs of $CI(S,Se)_2$ absorbers annealed with heating rate set at a) 1.8°C/s, b) 2.4°C/s, c) 8.8°C/s after cyanide etching

The diffractograms of Fig. 4, and the graph of Fig.5 show that the CIS (112) diffracted intensity more than doubles for the sample heated at 1.8°C/s compared to the material heated at 2.4°C/s. It then stays at the same level when the sample is heated faster than 2.4°C/s. This proves that the CIS is better crystallized with a heating rate of 2.4°C/s compared to 1.8°C/s and reaches saturation for heating rates above 2.4°C/s. The diffractogram of the sample heated at 8.8°C/s is not shown here for clarity but is very much alike to the one heated at 2.4°C/s. The same behavior is observed regarding the evolution of the crystallites size which is around 180nm after annealing with 1.8°C/s heating rate and increases to 220nm for heating rates faster than 2.4°C/s (Fig. 5).

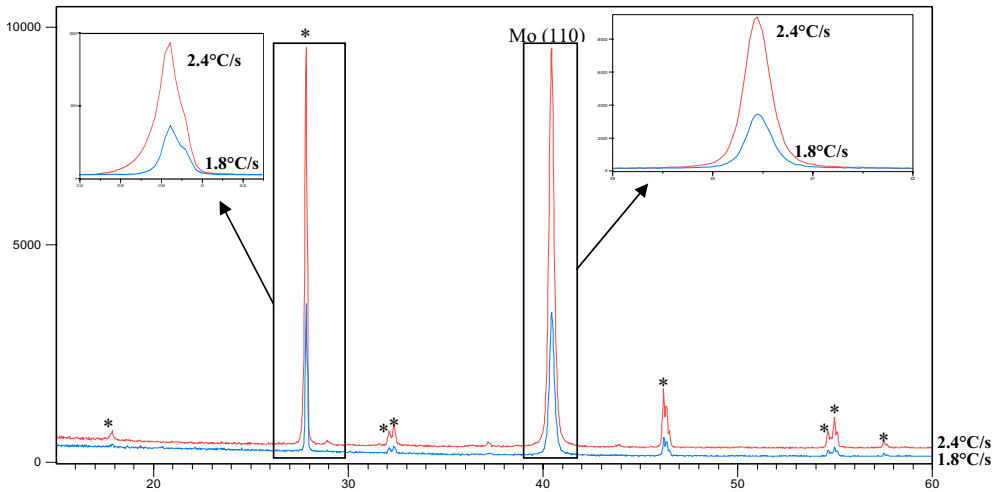

Fig. 4 :X-Ray diffractograms of samples annealed at 550°C with heating rate equal to 1.8°C/s and 2.4°C/s. CIS phase is marked with asterisks

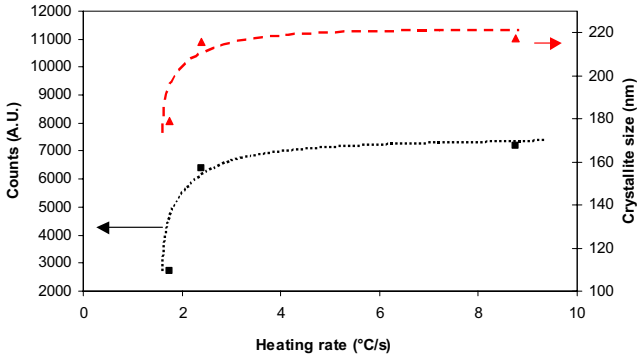

Fig. 5 : Evolution of CIS (112) reflection XRD intensity and evolution of the crystallites size inferred from Scherrer formula using the full width at half maximum FWHM of the (112) CIS reflection as a function of heating rate

Raman spectroscopy measurements of Fig. 6 show that the peak intensity of the A1 mode of Se-Se in $CuIn(S,Se)_2$ at $210cm^{-1}$ increases and the shoulder that can be assigned to CuAu ordered phase contribution at $305cm^{-1}$ decreases when the material is heated faster. The CuAu polytype evolution proves that the crystalline quality of the chalcopyrite improves when the material is heated faster.

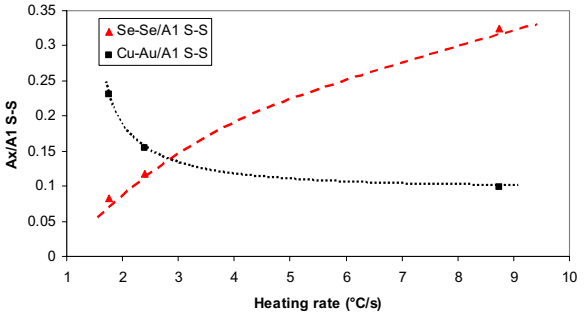

Fig. 6 : Dependence of the A1 Se-Se and CuAu ordered Raman contributions over the A1 S-S chalcopyrite as a function of heating rate

There is more selenium left in the absorber when the heating rate is higher (Fig. 6). This can be explained by considering the annealing mechanisms described elsewhere [7], which suggest that free selenium is lost by evaporation for T>250°C and that CuSe binaries decompose in $Cu_{2-x}Se$ and Se during the heating above 380°C and so the longer the annealing, the more selenium evaporates. Since the holding time was kept constant for all samples, then, when varying the heating rate, the total heating time was also modified ranging from 2 to 6 minutes. Therefore, a faster heating rate means a shorter total annealing time which explains that less selenium is lost. A higher concentration of selenium in the absorber then explains the larger grains noticed on Fig. 3 since it has been shown in [7] that CuSe binaries melting at 520°C tend to greatly enhance the film morphology.

As a consequence, the higher diffracted intensities for the CIS reflections of samples annealed at 2.4°C/s compared to those heated at 1.8°C/s can be explained considering that the faster the precursor is heated, the more selenium stays in the film which enables better morphology and an increase of the crystallites size.

An increase of the S-rich $Mo(S,Se)_2$ signal with the heating rate is detected on the Raman spectra in Fig. 7. Such a significant increase of the $Mo(S,Se)_2$ signal with the heating rate is rather surprising since the growth of this layer is known to be controlled by diffusion of chalcogens into the molybdenum [12], and thus should be controlled by annealing time and temperature [13] rather than heating rate.

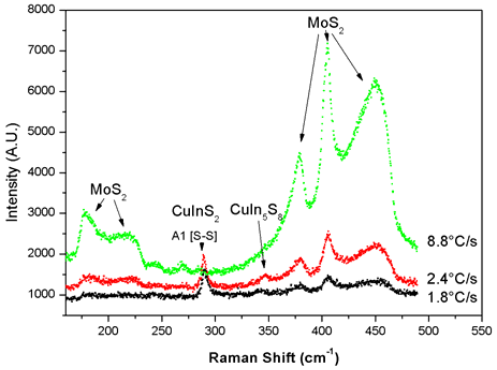

Fig. 7 : Cross Section Raman spectra obtained on absorbers heated at 1.8°C/s ; 2.4°C/s and 8.8°C/s showing the presence of MoS_2

The increase of the $Mo(S,Se)_2$ is confirmed by XRD analysis showing that an increase of the heating rate triggers an augmentation of the diffracted intensity for the (100) reflection of the hexagonal $Mo(S,Se)_2$ at 32.7°. The increase is, however, much less obvious on XRD diffractograms than that observed on the Raman spectra. The very high intensities observed in Raman spectra are actually due to a resonance phenomenon between the excitation laser and the vibration modes of the MoS_2. This explains why Raman spectroscopy is more sensitive than XRD to detect

MoS_2 variations. More information regarding the resonance phenomenon can be found in [14]. The increase of Raman and diffracted $Mo(S,Se)_2$ signals with the heating rate could be explained either considering that, when heated faster, the strain rate imposed on the molybdenum by the glass substrate due to thermal expansion mismatch is higher which can support diffusion of chalcogens in the molybdenum or because the sulfur pressure increases more rapidly when the heating rate is faster. Further studies are to be conducted to clarify the mechanisms behind this phenomenon.

3.3. Effect of sulfur concentration

Precursors were annealed at 650°C with a heating rate of 2.1°C/s and sulfur concentration varying from 10 mg/L to 1g/L. SEM cross-section micrographs taken on samples annealed with sulfur concentration of 33 mg/L and 400 mg/L show that a higher sulfur concentration results in a morphology with smaller grains Fig. 8.

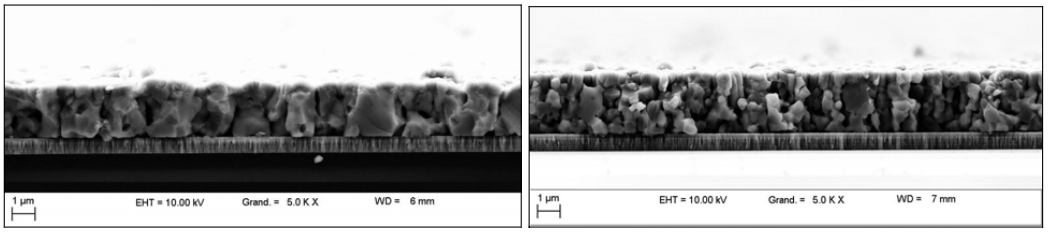

a) b)

Fig. 8 : SEM cross-section micrographs of $CuIn(S,Se)_2$ after cyanide etching annealed with sulfur concentration equal to a) 33 mg/L and b) 400 mg/L

Raman spectroscopy and X-Ray diffraction analysis was used to reveal the structural differences caused by an increase of sulfur concentration on the absorber. In the Raman spectra, the A1[Se-Se], A1[S-S] and $CuIn_5S_8$ Raman peaks shift towards higher wavenumber when the sulfur concentration increases (Fig. 9). Besides, although the lowest amount of sulfur used is already stoichiometrically sufficient to completely replace the selenium in the layer, there is a significant Raman signal corresponding to Se-Se vibration modes of the chalcopyrite visible for the lower sulfur concentrations which disappears when the sulfur concentration increases. This means that the more sulfur is added to the precursor before annealing the more sulfur is incorporated to the absorber after RTP and can reach almost pure $CuInS_2$. This observation is confirmed by the XRD analysis in [15] that shows that the (112) d-spacing of the chalcopyrite crystal can shift from the pure $CuInSe_2$ value at 3.34Å to almost pure $CuInS_2$ value at 3.20Å according to the sulfur quantity used.

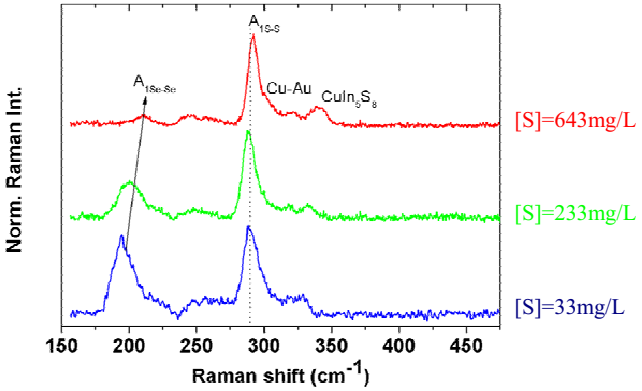

Fig. 9 : Representative Raman spectra of samples annealed with respectively 33, 233 and 643 mg/L sulfur concentration

Complete sulfurization of the absorber, when the sulfur quantity increases, is accompanied by a decrease of the FWHM for the A1 [S-S] mode of the chalcopyrite (Fig. 10) and a decrease of the relative area of the A1 [Se-Se] contribution (Fig. 11). The decrease of the FWHM shows that the crystalline quality of the S-rich $CuIn(S,Se)_2$ improves when the sulfur concentration increases up to 273 mg/L and then stays the same for higher sulfur values corresponding to completely sulfurized absorbers.

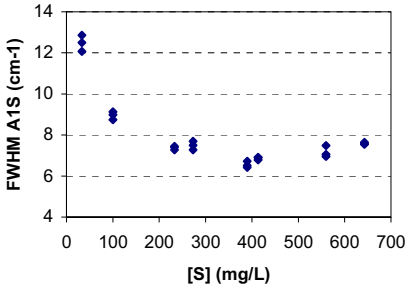

Fig. 10 : FWHM of $A_{1S\text{-}S}$ mode of Raman spectra as a function of the sulfur concentration

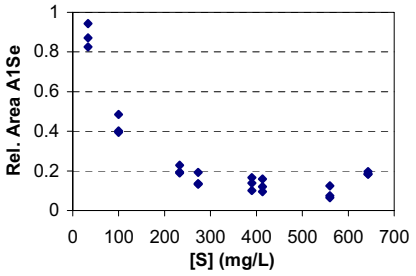

Fig. 11 : Relative area of A1Se-Se mode of Raman spectra as a function of the sulfur concentration

The decrease of the A1 [Se-Se] over A1 [S-S] ratio is in good agreement with the micrographs of Fig. 8 and observations from the previous paragraph which states that higher amount of selenium in the absorber results in a more coarsened morphology. However, increased coarsening is usually associated with better crystalline quality of the chalcopyrite which is not the case here since the FWHM of the A1 mode of the S-rich $CuIn(S,Se)_2$ chalcopyrite phase is lower for samples having a higher sulfur content. This phenomenon can be understood by taking into account that, for the lower concentration used, there is not enough sulfur incorporated in the absorber to produce homogeneous and well-crystallized S-rich $CuIn(S,Se)_2$. Morphology coarsening and crystalline quality improving are thus linked phenomena but the presence of the former does not necessarily trigger the latter.

The increase of the sulfur concentration results in an increase of the detrimental secondary phases such as CuAu ordered CIS and $CuIn_5S_8$ spinel-type structure (Fig. 12 a) and b)). Increasing the sulfur concentration from 10mg/L to 1g/L also resulted in an increase of the $Mo(S,Se)_2$ layer thickness from 110nm to 220nm as seen on SEM observations.

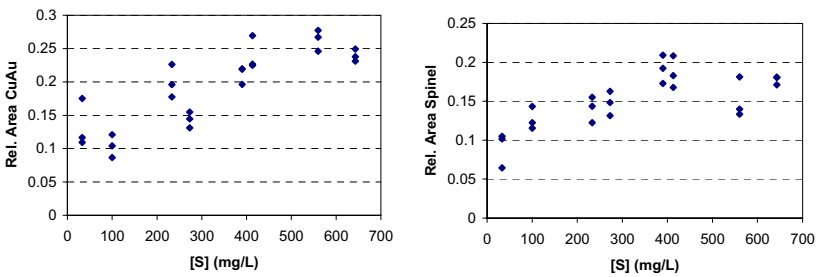

a) b)

Fig. 12: Relative Area of a) the CuAu ordered phase and b) the $CuIn_5S_8$ over the CIS chalcopyrite as a function of the sulfur concentration calculated from Raman spectroscopy measurements

Conclusions

This work demonstrated that morphological and structural properties of the absorber are very dependent on the RTP parameters such as annealing temperature, heating rate and sulfur concentration. A higher temperature causes primarily an increase in CIS grain size with a higher (112) preferential crystallographic orientation which is consistent with preferential grain growth where (112)-oriented crystallites are energetically favored compared to other orientations. The interfacial $Mo(S,Se)_2$ layer which grows due to sulfur and selenium diffusion into the molybdenum shows stronger signals as exhibited by Raman spectroscopy and X-Ray diffraction when the temperature increases but also when the heating rate increases. Temperature dependence was expected due to its formation mechanism by diffusion but the heating rate dependence needs more investigation to elucidate how the heating rate influences the formation of this layer. An increase of the heating rate results also in an increase in the CIS grain size and a better crystalline quality of the chalcopyrite with less Cu-Au ordered phase present. This improvement may be due to less selenium being lost when the material is heated faster and it is known that elemental Se and CuSe binaries present in the absorber during annealing have a positive impact on crystalline quality and morphology. Eventually, sulfur concentration in the reaction chamber has an effect on the sulpho-selenide concentration in the $CuIn(S,Se)_2$ absorber and also on the amount of detrimental secondary phases such as Cu-Au ordered phase or spinel-type structure. These results helped to better understand how RTP parameters influence the structure and morphology of the absorber which in turn will enable a better control of the final properties of the solar cells.

References:

[1] C.A. Kaufman et al., Thin Solid Films 515 (2007) 6217–6221
[2] R. Scheer et al., Solar Energy 77 (2004) 777–784
[3] M. Krunksa et al. , Thin Solid Films 361-362 (2000) 61-64
[4] D. Lincot et al., Solar Energy 77 (2004) 725-737
[5] I. Repins et al., Prog. Photovolt. Res. Appl. 16 (2008) 235
[6] E. Saucedo et al., Thin Solid Films, 517 (2009) 2268-2271
[7] A. Gobeaut et al., Thin Solid Films 517 (2009) 4436-4442
[8] V. Izquiedo-Roca et al., J. Appl. Phys. 101, (2007) 103517
[9] S. Karim et al., Appl. Phys A, 84, (2006) 403–407
[10] D. Abou-Ras et al., Thin Solid Films 517 (2009) 2545-2549
[11] V. Izquierdo-Roca et al., J. Appl. Phys. 103, (2008) 123109
[12] D. Abou-Ras et al., Thin Solid Films 480–481 (2005) 433–438
[13] V. Izquierdo-Roca et al., Thin Solid Films, 517 (2009) 2264-2267
[14] G.L. Frey et al., Phys. Rev. B 60 (1999) 2883
[15] S. Taunier et al., Thin Solid Films,480-481 (2005) 526-531